



## OPEN ACCESS

## EDITED BY

Feilong Zhang,  
Nanyang Technological University,  
Singapore

## REVIEWED BY

Shuqi Wang,  
Suzhou Institute of Nano-tech and  
Nano-bionics (CAS), China  
Yongchao Song,  
Qingdao University, China

## \*CORRESPONDENCE

Lingyan Zhang,  
18819818005@163.com  
Yibiao Liu,  
liuyibiao12345@126.com

\*These authors have contributed equally  
to this work

## SPECIALTY SECTION

This article was submitted to  
Biomaterials,  
a section of the journal  
Frontiers in Bioengineering and  
Biotechnology

RECEIVED 27 August 2022

ACCEPTED 07 October 2022

PUBLISHED 18 October 2022

## CITATION

Huang Z, Li M, Zhang L and Liu Y (2022),  
Electrochemical immunosensor based  
on superwetable microdroplet array for  
detecting multiple Alzheimer's  
disease biomarkers.  
*Front. Bioeng. Biotechnol.* 10:1029428.  
doi: 10.3389/fbioe.2022.1029428

## COPYRIGHT

© 2022 Huang, Li, Zhang and Liu. This is  
an open-access article distributed  
under the terms of the [Creative  
Commons Attribution License \(CC BY\)](#).  
The use, distribution or reproduction in  
other forums is permitted, provided the  
original author(s) and the copyright  
owner(s) are credited and that the  
original publication in this journal is  
cited, in accordance with accepted  
academic practice. No use, distribution  
or reproduction is permitted which does  
not comply with these terms.

# Electrochemical immunosensor based on superwetable microdroplet array for detecting multiple Alzheimer's disease biomarkers

Zhen Huang<sup>1,2†</sup>, Mifang Li<sup>1†</sup>, Lingyan Zhang<sup>1\*</sup> and Yibiao Liu<sup>1,2\*</sup>

<sup>1</sup>Longgang District Central Hospital of Shenzhen, Shenzhen, China, <sup>2</sup>Office of Shenzhen Clinical College, Guangzhou University of Chinese Medicine, Longgang District Central Hospital, Shenzhen, China

Alzheimer's disease (AD) is a neurodegenerative disease caused by neurons damage in the brain, and it poses a serious threat to human life and health. No efficient treatment is available, but early diagnosis, discovery, and intervention are still crucial, effective strategies. In this study, an electrochemical sensing platform based on a superwetable microdroplet array was developed to detect multiple AD biomarkers containing A $\beta$ 40, A $\beta$ 42, T-tau, and P-tau181 of blood. The platform integrated a superwetable substrate based on nanoAu-modified vertical graphene (VG@Au) into a working electrode, which was mainly used for droplet sample anchoring and electrochemical signal generation. In addition, an electrochemical micro-workstation was used for signals conditioning. This superwetable electrochemical sensing platform showed high sensitivity and a low detection limit due to its excellent characteristics such as large specific surface, remarkable electrical conductivity, and good biocompatibility. The detection limit for A $\beta$ 40, A $\beta$ 42, T-tau, and P-tau181 were 0.064, 0.012, 0.039, and 0.041 pg/ml, respectively. This study provides a promising method for the early diagnosis of AD.

## KEYWORDS

superwetable electrochemical biosensor, vertical graphene, gold nanoparticles, Alzheimer's disease, portable biosensors

## Introduction

Alzheimer's disease (AD) is a long-term neurodegenerative disease, that places a heavy burden on individuals, families, and communities. (Scheltens et al., 2021). Up to now, no effective cure for AD is available. Early diagnosis and early intervention are still very effective and important measures. (Li et al., 2021; Scheltens et al., 2021; Alzheimer's Association 2022). At present, the gold standards for AD diagnosis are positron emission tomography (PET) and the level of biomarkers, including  $\beta$ -amyloid (A $\beta$ ) peptide and tau protein, in cerebrospinal fluid (CSF). (Marcus et al., 2014; Scheltens et al., 2021). However, AD diagnosis based on PET or CSF biomarkers is inapplicable to AD screening of the

general population due to its high cost and invasive nature. Early diagnosis of AD based on blood biomarkers has elicited increased attention in recent years, and many studies have shown that AD can be diagnosed by measuring quantitative blood biomarkers, such as A $\beta$ 40, A $\beta$ 42, T-tau, and P-tau181. (Nakamura et al., 2018; Startin et al., 2019; Kim et al., 2020a; Janelidze et al., 2020; Thijssen et al., 2021; Mielke et al., 2022; Moscoso et al., 2022; Rubin 2022). However, the physiological concentration of AD blood markers, such as A $\beta$ 40, A $\beta$ 42, T-tau, and P-tau181, is only at the picograms level per milliliter. This concentration exceeds the detection limit of the conventional enzyme-linked immunosorbent assay (ELISA). Therefore, developing low-cost, non-invasive, and highly-sensitive detection methods for AD blood biomarkers is essential. (Nakamura et al., 2018; Brazaca et al., 2020). Thus far, many analytical methods have been developed to measure AD biomarkers in the blood, and these include electrochemistry (Liu et al., 2015; Liu et al. 2022a; Liu et al. 2022b; Zhang et al., 2022), fluorescence (Li et al., 2018; Zhang and Tan 2022), colorimetry (Duan et al., 2020), surface enhanced Raman spectroscopy (SERS) (Ma et al., 2021; Yang et al., 2022), and field-effect transistors (Sun Sang et al., 2021). Among these methods, electrochemical biosensors have great potential for disease diagnosis due to their easy miniaturization, high sensitivity, and low cost.

Superwettable microchips integrate two extremes of superhydrophobicity and superhydrophilicity into a 2D micropatterns (Xu et al., 2019), and are widely applied in biological medicine (Popova et al., 2015; Leite et al., 2017) and biochemical analysis (Xu et al., 2015; Xu et al. 2017; Xu et al. 2018) due to their outstanding ability for patterning microdroplets. In biosensing, superwettable microchips have remarkable advantages, including good microdroplet anchoring ability, low sample usage, high throughput, and

enrichment ability. In addition, superwettable microchips can be combined with various signal output approaches, such as electrochemistry (Zhang et al., 2017; Song et al., 2019; Zhu et al., 2022), fluorescence (Chen et al., 2018), colorimetry (Hou et al., 2015; Xu et al., 2017; Zhang et al., 2021), and SERS (Song et al., 2018).

In this study, we integrated a superwettable substrate into an electrochemical biosensor, and developed a portable superwettable electrochemical sensing platform for the detection of multiple AD blood biomarkers. As shown in Figure 1, this portable sensing platform is composed of a superwettable sensing substrate, an electrochemical micro-workstation, and a smartphone. The superwettable substrate contains superhydrophilic microwell regions and superhydrophobic regions. The antibody of the target protein was fixed to the superhydrophilic microwell region by Au-S. Then, BSA was used to block the nonspecific binding sites. The peak current of differential pulse voltammetry (DPV) further decreased after binding with the target antigen. The peak current of DPV was recorded, and the target protein concentration was calculated according to the peak current change value. The electrochemical micro-workstation and smartphone were used to regulate and control electrochemical signals. The superwettable electrochemical sensing platform used a two-electrode system. Ag/AgCl electrode served as the reference and counter electrodes. NanoAu-modified vertical graphene (VG) was used as the working electrode. The design of the microdroplet system significantly reduced the use of the sample. A real picture of this portable sensing platform was shown in Supplementary Figure S1. The superwettable microchip also showed an enrichment ability in some ways, and decreased the detection limit (LOD). As a result, the superwettable electrochemical sensing platform exhibited a wide linear range

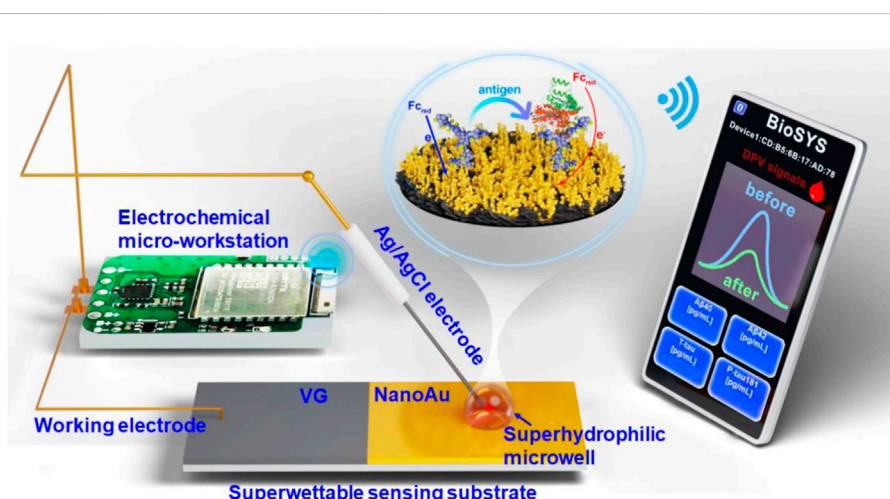


**FIGURE 1**  
Schematic of the superwettable electrochemical sensing platform for AD biomarkers.

and low LOD. This work offers great potential for the early diagnosis of AD.

## Experimental section

### Chemicals and materials

A $\beta$  peptides (including A $\beta$ 40 and A $\beta$ 42), human serum albumin (HSA), glucose (GLU), potassium chloride (KCl), potassium ferricyanide/ferrocyanide ( $K_3 [Fe(CN)_6]/K_4 [Fe(CN)_6]$ ), ferrocene, and phosphate-buffered solution (PBS, pH = 7.4, 10 mM) were purchased from Sigma-Aldrich (Shanghai, China). T-tau, P-tau181 protein, bovine serum albumin (BSA) and A $\beta$  antibody were purchased from Abcam Ltd (Hong Kong, China). The antibodies of T-tau and P-tau181 were obtained from Thermo Fisher Scientific Co., Ltd. (Beijing, China). The commercial goat serum (Gibco) was purchased from Thermo Fisher Scientific Co., Ltd. (Beijing, China). All chemical reagents were of analytical grade. All solutions were prepared with ultrapure water (Milli-Q, 18.2 M $\Omega$ ).

### Characterization and measurement

The morphology and elemental mapping of VG and VG modified with nanoAu were characterized through field-emission scanning electron microscopy (SEM, ThermoFisher, FEI Apreo S, Waltham, MA, United States). Water contact angles (CA) were measured at room temperature with a DSA100S system (KRUSS, Germany). All electrochemical measurements were performed on a customized electrochemical micro-workstation (Refresh AI Biosensor Co., Ltd., Shenzhen, China) at room temperature.

### Construction of superwetable electrochemical substrate

First, VG on a ceramic surface was prepared through chemical vapor deposition (CVD). Second, nanoAu was modified on the VG surface through the electrodeposition of 10 mM H $AuCl_4$ . The deposition voltage was -1.8 V, and deposition time was 300 s. Third, the VG substrate modified with nanoAu was immersed in a n-decanethiol solution for 24 h at room temperature, and n-decanethiol was fixed on the surface of nanoAu. Lastly, the nanoAu modified with n-decanethiol substrate was treated with 120 s O $_2$  plasma to obtain a superwetting electrochemical substrate containing superhydrophobic and superhydrophilic regions.

### Preparation of electrochemical sensing platform based on superwetable substrate

After preparing the superwetable substrate, a superwetable electrochemical biosensor was constructed. First, 5  $\mu$ L of the

antibody of target protein (A $\beta$ 40, A $\beta$ 42, T-tau, and P-tau181) was dripped onto the superhydrophilic microwell region and incubated at 37°C for 1 h. Second, 5  $\mu$ L of bovine serum albumin (BSA, 1%) was dropped onto the microwell, which was incubated for 1 h, and used to block the nonspecific binding sites. Third, 5  $\mu$ L of different concentrations of the target protein was added to the superhydrophilic microwell surface, and incubated for 1 h at 37°C. After each step, the microwell surface was washed three times with PBS (0.01 M, pH = 7.4). Lastly, by combining the superwetable electrochemical substrate with the electrochemical micro-workstation, a superwetable electrochemical sensing platform was successfully constructed.

The target protein was measured *via* DPV by using a portable electrochemical micro-workstation. The working potential of DPV was in the range of 0–0.4 V. After incubation with different concentrations of the target protein, the corresponding peak current change value ( $\Delta I$ ) was recorded, and used to calculate the concentration of the target protein. The selectivity of this superwetable electrochemical sensing platform was investigated in PBS buffer containing HSA, GLU, A $\beta$ 40, A $\beta$ 42, Tau441, and P-tau181.

### The application of the superwetable electrochemical sensing platform in goat serum.

The performance of the portable superwetable electrochemical sensing platform in goat serum was characterized through DPV. In brief, the antibody of the target protein (5  $\mu$ L) was immobilized on the superhydrophilic microwell surface. Then 5  $\mu$ L of commercial serum samples (1  $\mu$ L goat serum diluted with 4  $\mu$ L PBS buffer) containing different concentrations of the target protein (1, 10, and 100 pg/ml) was added to each superhydrophilic microwell surface and incubated at 37°C for 1 h. The peak current change value of the DPV signal was monitored in this process.

### Detection of clinical serum samples

5  $\mu$ L clinical human sample (1  $\mu$ L sample diluted with 4  $\mu$ L PBS buffer) was added to the superhydrophilic microwell surface and incubated for 1 h at 37°C. The peak current value of DPV signals was recorded, and the target protein concentration was calculated according to the peak current changing value.

## Results and discussion

### Preparation and characterization of superwetable substrate

The fabrication of the superwetable substrate is shown in [Supplementary Figure S2](#). NanoAu was modified on the surface by electrodeposition, which could increase the electron transfer rates and improve the sensitivity of the sensor. N-decanethiol was immobilized on the nanoAu surface, and the water contact angle

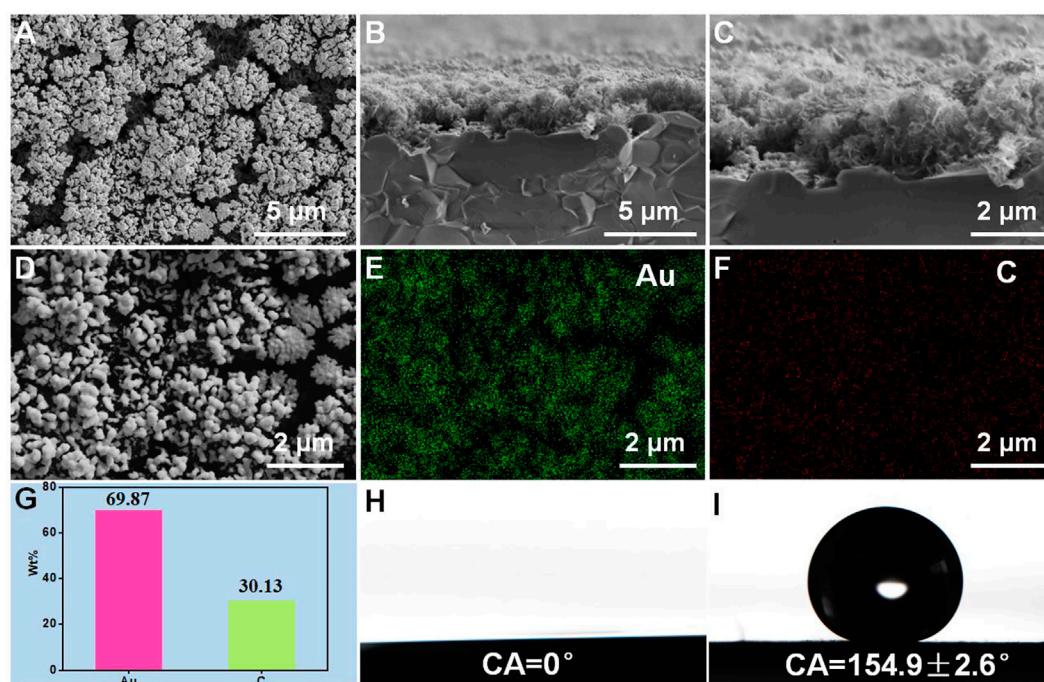


**FIGURE 2**  
Surface (A) and cross-section view (B,C) SEM images of vertical graphene modified with nanoAu. Surface element distribution characterization (D–G) of vertical graphene modified with nanoAu. Water contact angles of the superhydrophilic region (H) and superhydrophobic region (I).

was  $154.9 \pm 2.6^\circ$ , indicating a superhydrophobic surface. After treatment by  $O_2$  plasma for 120 s, the water contact angle became  $0^\circ$ , indicating that the region without photomask became superhydrophilic. (Figures 2H,I). A superwetable substrate that included superhydrophobic and superhydrophilic regions was successfully prepared.

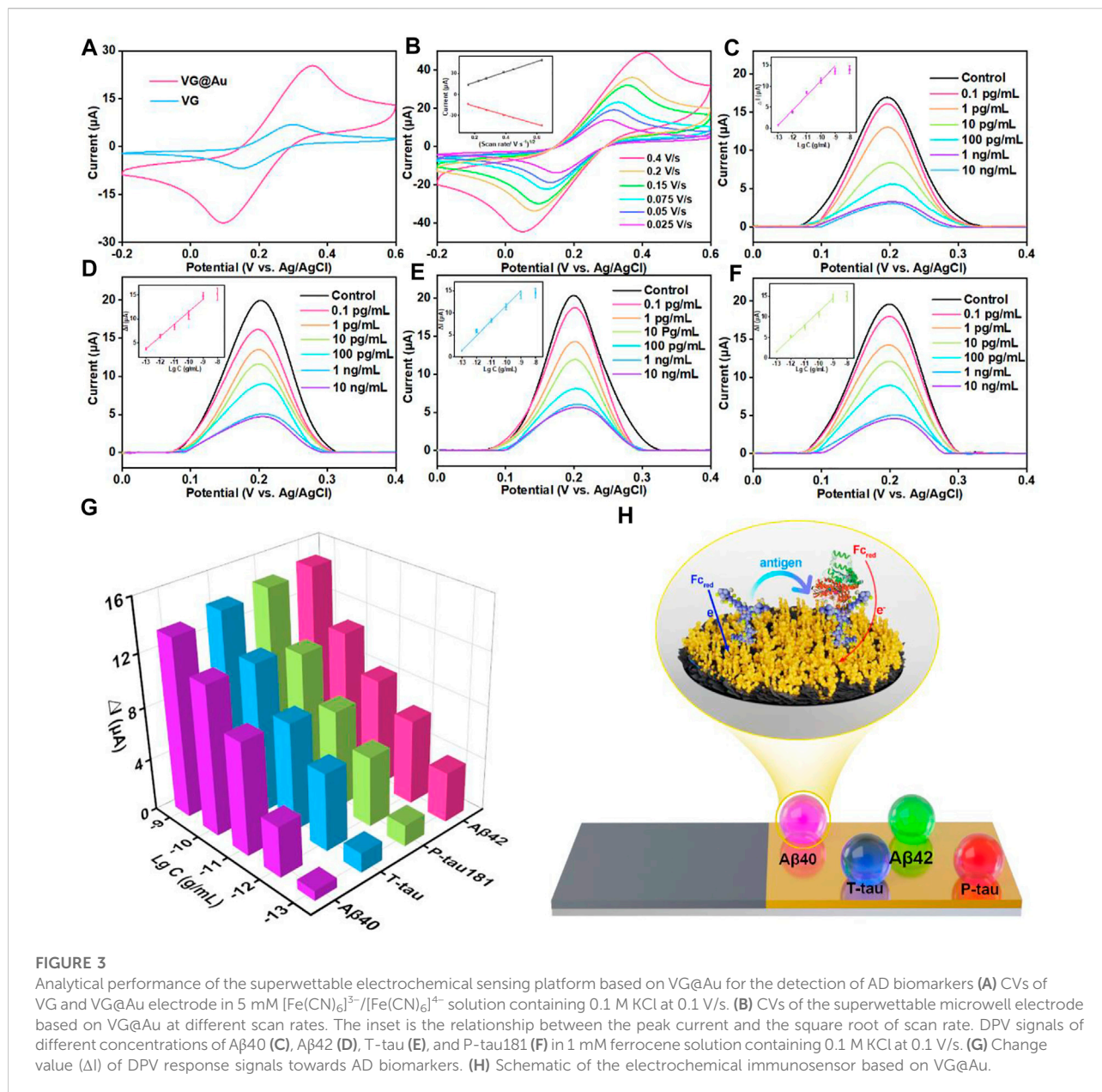
The surface morphology of the superwetable substrate was evaluated *via* SEM, and the results are shown in Figure 2A. Many gold nanoparticles were observed on the surface of the layered vertical graphene structures. The cross-section view SEM images of vertical graphene was shown in Supplementary Figure S3. The cross-section view morphology of vertical graphene@Au is shown in Figures 2B,C. The gold nanoparticles were deposited mainly on the VG surface. In addition, the content of Au was measured through energy dispersive X-ray (EDX), and the result showed that the weight percent of Au element was 69.87%, indicating that most of the surface areas of VG were covered with Au nanoparticles (Figures 2D–G).

## Construction and analytical performance of superwetable electrochemical sensing platform

The electroactive areas of VG and VG@Au were compared by cyclic voltammetry (CVs), and the results showed that the

electroactive area of the VG@Au electrode was remarkably larger than that of the VG electrode. (Figure 3A). In addition, the electrode surface dynamics process was evaluated by CV at different scan rates. As shown in Figure 3B, the peak current had a linear relation with the square root of the scan rate, indicating a diffusion-limited process. After the superwetable substrate was completed, the antibody of the target protein ( $A\beta_{40}$ ,  $A\beta_{42}$ , T-tau, and P-tau181) was immobilized on the superhydrophilic microwell region by Au-S. After modifying the corresponding antibody, the peak current of the DPV signal decreased, which indicated that the target protein antibody was successfully fixed on the superwetable microwell region surface (Supplementary Figure S4, lines I and II). Then, BSA was used to block the nonspecific adsorption sites, and the peak current of the DPV signals further decreased (Supplementary Figure S4, line III). Afterward, the different concentrations of the target protein were added to the superhydrophilic microwell region surface. During this period, the DPV signal was recorded, and the concentration of the target protein was calculated based on the variation of the peak current.

The concentration of the target protein antibody was optimized before the final test. As shown in Supplementary Figure S5, the optimized concentration of the target protein antibody was  $10 \mu\text{g/ml}$ . Under the optimized condition, the antibody of four proteins was immobilized in the



superhydrophilic microwell regions, and the concentration of the target proteins was measured by the variation in the resistance of the superhydrophilic microwell region surface, as shown in Figure 3H. The corresponding antibody specifically recognized the target protein (A $\beta$ 40, A $\beta$ 42, T-tau, and P-tau181), resulting in the increase in surface resistance, which caused signal reduction. The peak current of the DPV signals was recorded by the electrochemical micro-workstation platform, and the concentration of the target protein was calculated by the variation in peak current.

As shown in Figures 3C–G, for the target protein (A $\beta$ 40, A $\beta$ 42, T-tau, and P-tau181), the peak current of DPV signals

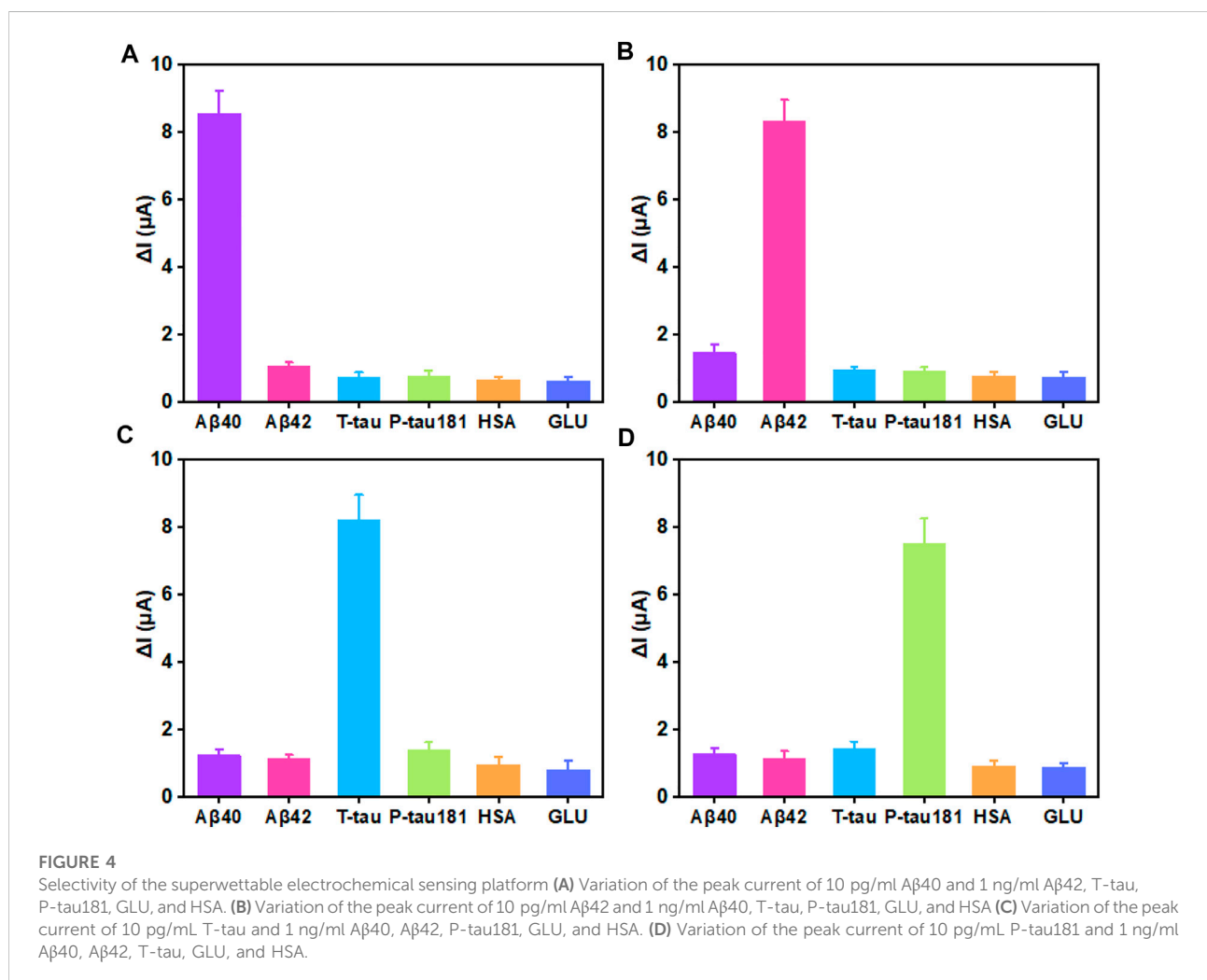
decreased, and the variation in peak current ( $\Delta I$ ) increased as the concentration of the target protein increased.  $\Delta I$  had a good linear relationship with the logarithm of target protein concentration from 0.1 pg/ml to 1,000 pg/ml. The detection limit of this superwetable electrochemical sensing platform for A $\beta$ 40 was about 0.064 pg/ml ( $S/N = 3$ ). The LOD was calculated as three times the standard deviation of the blank. (Chiavaioli et al., 2017; Esposito et al., 2021). Similarly, the LOD for A $\beta$ 42, T-tau, and P-tau181 was 0.012, 0.039, and 0.041 pg/ml, respectively.

In blood, the physiological concentration of A $\beta$ 40, A $\beta$ 42, T-tau, and P-tau181 was about several to hundreds of picograms per

TABLE 1 Comparison between the superwetttable electrochemical sensing platform and other sensors for the detection of AD biomarkers.

Method	Target	Detection limit	References
Electrochemistry	Tau, p-tau181, A $\beta$ 42, A $\beta$ 40	2.45, 2.72, 2.13, 2.20 fM	Kim et al. (2020b)
Electrochemistry	ApoE4, Tau, A $\beta$	$5.91 \times 10^{-11}$ ; $7.1 \times 10^{-11}$ ; $8.6 \times 10^{-12}$ mg/ml	Song et al. (2020)
Electrochemistry	T-tau, p-tau181, A $\beta$ 40, A $\beta$ 42	0.125, 0.089, 0.142, 0.176 pg/ml	Liu et al. (2022a)
Fluorescence	A $\beta$ 42, tau441, p-tau181	340.07, 669.44, 493.79 pg/ml	Chan et al. (2017)
LSPR	A $\beta$ 40, A $\beta$ 42, T-tau,	34.9, 26, 23.6 fM	Kim et al. (2018)
SERS	Tau, A $\beta$ 42 oligomers	$4.2 \times 10^{-4}$ pM, $3.7 \times 10^{-2}$ nM	Zhang et al. (2019)
FET sensor	tau	10 fg/ml	Sun Sang et al. (2021)
Electrochemistry	T-tau, p-tau181, A $\beta$ 40, A $\beta$ 42	0.039, 0.041, 0.064, 0.012 pg/ml	This work

Selectivity and stability.



milliliter. This result shows that our developed superwetttable electrochemical sensing platform satisfies the needs of detecting AD biomarkers in blood. The superwetttable electrochemical sensing platform based on the VG@Au array exhibited a low LOD and a

wide linear range. A comparison of this method and methods in previous reports is shown in Table 1. Our developed superwetttable electrochemical sensing platform exhibited excellent analytical performance. The concentration of AD biomarkers including

A $\beta$ 40, A $\beta$ 42, T-tau, and P-tau181, was at picograms per milliliter of blood. The LOD of this superwetable electrochemical sensing platform was lower than 0.1 pg/ml, which meets the requirements for the detection of AD biomarkers.

## Selectivity and stability

In biological application, selectivity and stability are important factors for biosensors. The selectivity and stability of this superwetable electrochemical sensing platform were investigated. As shown in [Figure 4A](#), when 10 pg/ml of A $\beta$ 40 was added, an obvious signal response of 8.56  $\mu$ A was obtained. On the surface of the superhydrophilic microwell sensing region, the concentration of other proteins including A $\beta$ 42, T-tau, P-tau181, GLU, and HSA was 100-fold higher than that of A $\beta$ 40, and the  $\Delta I$  for A $\beta$ 42, T-tau, P-tau181, GLU, and HSA was 1.06, 0.73, 0.75, 0.66, and 0.62  $\mu$ A, respectively, which accounted for 12.4%, 8.5%, 8.7%, 7.7%, and 7.2% of the  $\Delta I$  for A $\beta$ 40, respectively. For A $\beta$ 42 sensing region, the signal response was about 8.33  $\mu$ A. The  $\Delta I$  for A $\beta$ 40, T-tau, P-tau181, GLU, and HSA was 1.46, 0.96, 0.89, 0.78, and 0.73  $\mu$ A, respectively, which accounted for 17.5%, 11.5%, 10.6%, 9.3% and 8.7% of the  $\Delta I$  for A $\beta$ 42, respectively ([Figure 4B](#)). Likewise, for T-tau or P-tau181, the corresponding superhydrophilic microwell sensing region also displayed excellent selectivity ([Figures 4C,D](#)). These results indicate that the selectivity of this superwetable electrochemical sensing platform for A $\beta$ 40, A $\beta$ 42, T-tau, and P-tau181 was outstanding. In addition, the stability of this superwetable electrochemical sensing platform was evaluated by detecting six times of 10 pg/ml of the target protein (A $\beta$ 40, A $\beta$ 42, T-tau, and P-tau181) As shown in [Supplementary Figure S6](#), the sensor was stored in dry conditions at 4°C for 2 weeks. The  $\Delta I$  value still remained above 90% of its initial value after 14 days, demonstrating the acceptable stability of this superwetable electrochemical sensing platform based on VG@Au. The results prove that our developed electrochemical sensing platform based on a superwetable microarray has good stability and specificity.

## Application of this superwetable electrochemical sensing platform in serum sample

To further evaluate the clinical application of the superwetable electrochemical sensing platform, goat serum samples that included A $\beta$ 40, A $\beta$ 42, T-tau, and P-tau181 were detected by using the designed superwetable platform. The diluted serum samples were spiked with different concentrations of the target protein (1, 10, and 100 pg/ml) including A $\beta$ 40, A $\beta$ 42, T-tau, and P-tau181. The result was shown in [Supplementary Table S1](#). No significant difference was observed between the detected and added values. The recovery rate ranged

from 91% to 109.1%. In addition, we conduct two clinical samples and compared the results with the results from typical ELISA. As shown in [Supplementary Table S2](#), A $\beta$ 40 and A $\beta$ 42 can be detected by this superwetable sensor and typical ELISA, there was no significant difference between the result of our sensor and that of ELISA. This result demonstrated that our developed superwetable electrochemical sensing platform based on VG@Au could be used for detecting the clinical samples. What's more, T-tau and P-tau181 were detected by this sensor, but they were not detected by typical ELISA, indicating that this superwetable electrochemical sensor has lower LOD. To sum up, the superwetable electrochemical sensing platform based on VG@Au has excellent sensitivity and reliability for the detection of AD biomarkers in clinical serum sample analysis, and could be capable of clinical diagnosis.

## Conclusion

In summary, a portable superwetable electrochemical sensing platform based on the VG@Au substrate was designed and constructed to detect multiple AD biomarkers in serum. The superwetable VG@Au substrate included superhydrophobic and superhydrophilic regions on the VG@Au surface, which could be used for fixing a microdroplet sample, and used as a working electrode to generate electrochemical signals. In addition, an electrochemical micro-workstation was introduced to this superwetable electrochemical sensing platform to adjust the signal. The superwetable electrochemical sensing platform based on the superwetable VG@Au substrate showed excellent analytical performance with a low detection limit and high sensitivity due to the good properties of VG@Au, including large specific surface, outstanding electrical conductivity, and good biocompatibility. As a result, the detection limit for A $\beta$ 40, A $\beta$ 42, T-tau, and P-tau181 were 0.064, 0.012, 0.039, and 0.041 pg/ml, respectively. In blood, the AD biomarker concentration was at the  $\sim$ pg/mL level. Our designed superwetable sensing platform satisfies the need for detection in blood. This work offers a new method of detecting AD biomarkers in serum. The method exhibits great potential for early diagnosis of AD.

## Data availability statement

The original contributions presented in the study are included in the [article/Supplementary Material](#), further inquiries can be directed to the corresponding authors.

## Author contributions

YL and LZ provide the idea, design the experiment, and write the paper. ZH and ML mainly do the experiment and analyze data.

## Funding

This work was supported by the medical and health technology plan project of special fund for economic and technological development of longgang district, Shenzhen, PR. China (Grant no. LGKCYLWS2020001), Longgang District Medical and health science and technology project (grant no. LGKCYLWS2021000003).

## Acknowledgments

We thank the Instrumental Analysis Center of Shenzhen University (Xili Campus) for providing access to the instruments used in the experiments. We thank the advice of Jianbo Yu.

## References

- Alzheimer's Association (2022). Alzheimer's disease facts and figures. *Alzheimers Dement.* 1–90. doi:10.1002/alz.12638
- Brazaca, L. C., Sampaio, I., Zucolotto, V., and Janegitz, B. C. (2020). Applications of biosensors in Alzheimer's disease diagnosis. *Talanta* 210, 120644. doi:10.1016/j.talanta.2019.120644
- Chan, H. N., Xu, D., Ho, S. L., Wong, M. S., and Li, H. W. (2017). Ultra-sensitive detection of protein biomarkers for diagnosis of Alzheimer's disease. *Chem. Sci.* 8, 4012–4018. doi:10.1039/c6sc05615f
- Chen, Y., Xu, L.-P., Meng, J., Deng, S., Ma, L., Zhang, S., et al. (2018). Superwetable microchips with improved spot homogeneity toward sensitive biosensing. *Biosens. Bioelectron.* 102, 418–424. doi:10.1016/j.bios.2017.11.036
- Chiavaioli, F., Gouveia, C. A. J., Jorge, P. A. S., and Baldini, F. (2017). Towards a uniform metrological assessment of grating-based optical fiber sensors: From refractometers to biosensors. *Biosensors* 7, 23. doi:10.3390/bios7020023
- Duan, C., Jiao, J., Zheng, J., Li, D., Ning, L., Xiang, Y., et al. (2020). Polyvalent biotinylated aptamer scaffold for rapid and sensitive detection of tau proteins. *Anal. Chem.* 92, 15162–15168. doi:10.1021/acs.analchem.0c03643
- Esposito, F., Sansone, L., Srivastava, A., Baldini, F., Campopiano, S., Chiavaioli, F., et al. (2021). Long period grating in double cladding fiber coated with graphene oxide as high-performance optical platform for biosensing. *Biosens. Bioelectron.* 172, 112747. doi:10.1016/j.bios.2020.112747
- Hou, J., Zhang, H., Yang, Q., Li, M., Jiang, L., and Song, Y. (2015). Hydrophilic-hydrophobic patterned molecularly imprinted photonic crystal sensors for high-sensitive colorimetric detection of tetracycline. *Small* 11, 2738–2742. doi:10.1002/smll.201403640
- Janelidze, S., Mattsson, N., Palmqvist, S., Smith, R., Beach, T. G., Serrano, G. E., et al. (2020). Plasma P-tau181 in alzheimer's disease: Relationship to other biomarkers, differential diagnosis, neuropathology and longitudinal progression to alzheimer's dementia. *Nat. Med.* 26, 379–386. doi:10.1038/s41591-020-0755-1
- Kim, H., Lee, J. U., Song, S., Kim, S., and Sim, S. J. (2018). A shape-code nanoplasmonic biosensor for multiplex detection of Alzheimer's disease biomarkers. *Biosens. Bioelectron.* X, 101, 96–102. doi:10.1016/j.bios.2017.10.018
- Kim, K., Kim, M. J., Kim, D. W., Kim, S. Y., Park, S., and Park, C. B. (2020a). Clinically accurate diagnosis of Alzheimer's disease via multiplexed sensing of core biomarkers in human plasma. *Nat. Commun.* 11, 119. doi:10.1038/s41467-019-13901-z

## Conflict of interest

The authors declare that the research was conducted in the absence of any commercial or financial relationships that could be construed as a potential conflict of interest.

## Publisher's note

All claims expressed in this article are solely those of the authors and do not necessarily represent those of their affiliated organizations, or those of the publisher, the editors and the reviewers. Any product that may be evaluated in this article, or claim that may be made by its manufacturer, is not guaranteed or endorsed by the publisher.

## Supplementary material

The Supplementary Material for this article can be found online at: <https://www.frontiersin.org/articles/10.3389/fbioe.2022.1029428/full#supplementary-material>

- Kim, K., Lee, C. H., and Park, C. B. (2020b). Chemical sensing platforms for detecting trace-level Alzheimer's core biomarkers. *Chem. Soc. Rev.* 49, 5446–5472. doi:10.1039/d0cs00107d
- Leite, Á. J., Oliveira, M. B., Caridade, S. G., and Mano, J. F. (2017). Screening of nanocomposite scaffolds arrays using superhydrophobic-wettable micropatterns. *Adv. Funct. Mat.* 27, 1701219. doi:10.1002/adfm.201701219
- Li, Y., Haber, A., Preuss, C., John, C., Uyar, A., Yang, H. S., et al. (2021). Alzheimer's Disease Neuroimaging, ITransfer learning-trained convolutional neural networks identify novel MRI biomarkers of Alzheimer's disease progression. *Alzheimers Dement.* 13, e12140. doi:10.1002/dad2.12140
- Li, Y., Wang, K., Zhou, K., Guo, W., Dai, B., Liang, Y., et al. (2018). Novel D-A-D based near-infrared probes for the detection of beta-amyloid and Tau fibrils in Alzheimer's disease. *Chem. Commun.* 54, 8717–8720. doi:10.1039/c8cc05259j
- Liu, Y., Huang, Z., Xu, Q., Zhang, L., Liu, Q., and Xu, T. (2022a). Portable electrochemical micro-workstation platform for simultaneous detection of multiple Alzheimer's disease biomarkers. *Microchim. Acta* 189, 91. doi:10.1007/s00604-022-05199-4
- Liu, Y., Liu, X., Li, M., Liu, Q., and Xu, T. (2022b). Portable vertical graphene@Au-based electrochemical aptasensing platform for point-of-care testing of tau protein in the blood. *Biosensors* 12, 564. doi:10.3390/bios12080564
- Liu, Y., Xu, L.-P., Wang, S., Yang, W., Wen, Y., and Zhang, X. (2015). An ultrasensitive electrochemical immunosensor for apolipoprotein E4 based on fractal nanostructures and enzyme amplification. *Biosens. Bioelectron.* 71, 396–400. doi:10.1016/j.bios.2015.04.068
- Ma, H., Liu, S., Liu, Y., Zhu, J., Han, X. X., Ozaki, Y., et al. (2021). *In-situ* fingerprinting phosphorylated proteins via surface-enhanced Raman spectroscopy: Single-site discrimination of Tau biomarkers in Alzheimer's disease. *Biosens. Bioelectron.* 171, 112748. doi:10.1016/j.bios.2020.112748
- Marcus, C., Mena, E., and Subramaniam, R. M. (2014). Brain PET in the diagnosis of Alzheimer's disease. *Clin. Nucl. Med.* 39, e413–e426. quiz e423–416. doi:10.1097/RLU.0000000000000547
- Mielke, M. M., Dage, J. L., Frank, R. D., Algeciras-Schimnich, A., Knopman, D. S., Lowe, V. J., et al. (2022). Performance of plasma phosphorylated tau 181 and 217 in the community. *Nat. Med.* 28, 1398–1405. doi:10.1038/s41591-022-01822-2
- Moscoco, A., Karikari, T. K., Grothe, M. J., Ashton, N. J., Lantero-Rodriguez, J., Snellman, A., et al. (2022). CSF biomarkers and plasma p-tau181 as predictors of

- longitudinal tau accumulation: Implications for clinical trial design. *Alzheimers Dement.* doi:10.1002/alz.12570
- Nakamura, A., Kaneko, N., Villemagne, V. L., Kato, T., Doecke, J., Dore, V., et al. (2018). High performance plasma amyloid-beta biomarkers for Alzheimer's disease. *Nature* 554, 249–254. doi:10.1038/nature25456
- Popova, A. A., Schillo, S. M., Demir, K., Ueda, E., Nesterov-Mueller, A., and Levkin, P. A. (2015). Droplet-array (da) sandwich chip: A versatile platform for high-throughput cell screening based on superhydrophobic–superhydrophilic micropatterning. *Adv. Mat.* 27, 5217–5222. doi:10.1002/adma.201502115
- Rubin, R. (2022). New test to help diagnose alzheimer disease. *JAMA* 327, 2281. doi:10.1001/jama.2022.9847
- Scheltens, P., De Strooper, B., Kivipelto, M., Holstege, H., Chételet, G., Teunissen, C. E., et al. (2021). Alzheimer's disease. *Lancet* 397, 1577–1590. doi:10.1016/s0140-6736(20)32205-4
- Song, Y., Xu, T., Xu, L.-P., and Zhang, X. (2019). Nanodendritic gold/graphene-based biosensor for tri-mode miRNA sensing. *Chem. Commun.* 55, 1742–1745. doi:10.1039/C8CC09586H
- Song, Y., Xu, T., Xu, L.-P., and Zhang, X. (2018). Superwetable nanodendritic gold substrates for direct miRNA SERS detection. *Nanoscale* 10, 20990–20994. doi:10.1039/C8NR07348A
- Song, Y., Xu, T., Zhu, Q., and Zhang, X. (2020). Integrated individually electrochemical array for simultaneously detecting multiple Alzheimer's biomarkers. *Biosens. Bioelectron.* X. 162, 112253. doi:10.1016/j.bios.2020.112253
- Startin, C. M., Ashton, N. J., Hamburg, S., Hithersay, R., Wiseman, F. K., Mok, K. Y., et al. (2019). Plasma biomarkers for amyloid, tau, and cytokines in Down syndrome and sporadic Alzheimer's disease. *Alz. Res. Ther.* 11, 26. doi:10.1186/s13195-019-0477-0
- Sun Sang, K., Dongwoo, K., Mijin, Y., Jeong Gon, S., and Soo Hyun, L. (2021). The role of graphene patterning in field-effect transistor sensors to detect the tau protein for Alzheimer's disease: Simplifying the immobilization process and improving the performance of graphene-based immunosensors. *Biosens. Bioelectron.* 192, 113519. doi:10.1016/j.bios.2021.113519
- Thijssen, E. H., La Joie, R., Strom, A., Fonseca, C., Iaccarino, L., Wolf, A., et al. (2021). Plasma phosphorylated tau 217 and phosphorylated tau 181 as biomarkers in alzheimer's disease and frontotemporal lobar degeneration: A retrospective diagnostic performance study. *Lancet Neurology* 20, 739–752. doi:10.1016/s1474-4422(21)00214-3
- Xu, L. P., Chen, Y., Yang, G., Shi, W., Dai, B., Li, G., et al. (2015). Ultratrace DNA detection based on the condensing-enrichment effect of superwetable microchips. *Adv. Mat.* 27, 6878–6884. doi:10.1002/adma.201502982
- Xu, T., Li-Ping, X., Xueji, Z., and Shutao, W. (2019). Bioinspired superwetable micropatterns for biosensing. *Chem. Soc. Rev.* 48, 3153–3165. doi:10.1039/C8CS00915E
- Xu, T., Shi, W., Huang, J., Song, Y., Zhang, F., Xu, L.-P., et al. (2017). Superwetable microchips as a platform toward microgravity biosensing. *ACS Nano* 11, 621–626. doi:10.1021/acsnano.6b06896
- Xu, T., Song, Y., Gao, W., Wu, T., Xu, L.-P., Zhang, X., et al. (2018). Superwetable electrochemical biosensor toward detection of cancer biomarkers. *ACS Sens.* 3, 72–78. doi:10.1021/acssensors.7b00868
- Yang, S. J., Lee, J. U., Jeon, M. J., and Sim, S. J. (2022). Highly sensitive surface-enhanced Raman scattering-based immunosensor incorporating half antibody-fragment for quantitative detection of Alzheimer's disease biomarker in blood. *Anal. Chim. Acta* 1195, 339445. doi:10.1016/j.aca.2022.339445
- Zhang, H., Oellers, T., Feng, W., Abdulazim, T., Saw, E. N., Ludwig, A., et al. (2017). High-density droplet microarray of individually addressable electrochemical cells. *Anal. Chem.* 89, 5832–5839. doi:10.1021/acs.analchem.7b00008
- Zhang, K., Zhang, J., Wang, F., and Kong, D. (2021). Stretchable and superwetable colorimetric sensing patch for epidermal collection and analysis of sweat. *ACS Sens.* 6, 2261–2269. doi:10.1021/acssensors.1c00316
- Zhang, P., and Tan, C. (2022). Cross-reactive fluorescent sensor array for discrimination of amyloid beta aggregates. *Anal. Chem.* 94, 5469–5473. doi:10.1021/acs.analchem.2c00579
- Zhang, X., Liu, S., Song, X., Wang, H., Wang, J., Wang, Y., et al. (2019). Robust and universal SERS sensing platform for multiplexed detection of alzheimer's disease core biomarkers using PAapt-AuNPs conjugates. *ACS Sens.* 4, 2140–2149. doi:10.1021/acssensors.9b00974
- Zhang, Z.-h., Hu, J., Zhu, H., Chen, Q., Koh, K., Chen, H., et al. (2022). A facile and effective immunoassay for sensitive detection of phosphorylated tau: The role of flower-shaped TiO<sub>2</sub> in specificity and signal amplification. *Sensors Actuators B Chem.* 366, 132015. doi:10.1016/j.snb.2022.132015
- Zhu, Q., Yang, Y., Gao, H., Xu, L.-P., and Wang, S. (2022). Bioinspired superwetable electrodes towards electrochemical biosensing. *Chem. Sci.* 13, 5069–5084. doi:10.1039/D2SC00614F